

STRUCTURE AND MAGNETIC PROPERTIES OF Ni-C NANOCOMPOSITE

Yunasfi^{1*}, Wisnu Ari Adi¹

¹ Centre for Science and Technology of Advanced Materials – National Nuclear Energy Agency,
Kawasan Puspiptek Serpong, Tangerang Selatan, Banten, Indonesia

(Received: December 2015 / Revised: January 2016 / Accepted: January 2016)

ABSTRACT

The synthesis and characterization of nickel-graphite (Ni-C) nanocomposite materials by mechanical milling method have been performed. This composite was prepared by mixing high purity nickel and graphite. The mixture was milled for 25, 50, and 75 hours and then was compacted at pressure of 5000 psi. The samples consist of two phases, namely carbon and nickel phases. Carbon phase has hexagonal structure, space group: $P 6_3 m c$ (186), lattice parameters of $a = b = 2.352(1) \text{ \AA}$ and $c = 6.669(7) \text{ \AA}$, $\alpha = \beta = 90^\circ$ and $\gamma = 120^\circ$, $V = 31.9(7) \text{ \AA}^3$ and $\rho = 5.585 \text{ gr.cm}^{-3}$. Nickel phase has cubic structure, space group: $F m \bar{3} m$ (225), lattice parameters of $a = b = c = 3.5254(7) \text{ \AA}$, $\alpha = \beta = \gamma = 90^\circ$, $V = 43.81(2) \text{ \AA}^3$ and $\rho = 8.898 \text{ gr.cm}^{-3}$. The calculation results show that the crystallite size of the Ni-C75 sample was around 3.83 nm. The Ni-C75 sample is also suspected to have grown embryo of carbon nanotube (CNT) due to the presence of nickel. The hysteresis loop of the sample consists of intrinsic saturation M_s , remanence M_r , and coercivity H_c are 1.40 emu/gr, 0.28 emu/gr, and 128 Oe, respectively. The value of MR is about 28% at 7.5 kOe magnetic field. The sample shows magnetoresistance behavior and the phenomenon of sensor characteristics. We concluded that this study has successfully made Ni-C nanocomposite and it is expected that the nano composite Ni-C is able to be used for sensor material application.

Keywords: Crystallite Size; Magnetic; Magnetoresistance; Nanocomposite; Ni-C

1. INTRODUCTION

Graphite is the most stable form of carbon allotropes at standard conditions. Graphite has a layered planar structure. In each layer, the carbon atoms are arranged like a honeycomb lattice with a separation distance of 0.142 nm, and the distance between the planes was 0.335 nm (Mandal et al., 2013). There are two known forms of graphite, namely alpha graphite (hexagonal) and beta graphite (rhombohedral). Graphite can also conduct electricity due to extensive electron delocalization within the carbon layers. This phenomenon is called aromaticity. The valence electrons are free to move, so that they could conduct electricity (Sagar et al., 2014). Recent research suggests that an effect called magnetoresistance appears also in graphite and these interactions usually involve magnetic elements, such as Fe, Ni, and Co. The use of graphite is only limited by the tendency to facilitate the interaction between magnetic ions (Guler & Evin, 2012; Cernak et al., 2014; Zou et al., 2010).

Previous studies have been carried out the synthesis of Ni-C (Yunasfi, 2013) and Fe-C nanocomposites (Schinteie et al., 2014; Dillon et al, 2012). Fe-C system is very interesting to

*Corresponding author's email: yunasfi@gmail.com, Tel. +62-21-7270032, Fax. +62-21-7270033
Permalink/DOI: <http://dx.doi.org/10.14716/ijtech.v7i3.2826>

understand its properties of electricity and magnetism, and this material could potentially be applied as sensor materials, energy storage capacitors, and catalysts (Venkatesan et al., 2013; Jia et al., 2011). Nanocomposite and nanostructured carbon containing iron nanoparticles that can exhibit properties of electricity and magnetism were unique. Fe-C has been shown that the composite material is a useful material for electromagnetic applications in the form of thin layers (Xu et al., 2012; Sagar et al., 2014).

2. METHODOLOGY

The nanocomposite of Ni-C was synthesized by using milling method. The samples were made of high purity nickel and graphite powders from Merck product. Composite samples are prepared by composition C:Ni = 98:2 wt% at various milling time, namely, 25, 50, and 75 hours. The raw materials are mixed by using a high energy milling (HEM) type Spex 8000 for 10 hours at room temperature. The finely mixed powder was compacted at 5000 psi into pellets.

The qualitative and quantitative analysis of phases were carried out using Rigaku diffractometer with $\text{CuK}\alpha$ radiation ($\lambda = 1.5406 \text{ \AA}$). The Rietveld analysis was performed by applying GSAS software (Toby, 2000). Additional X-ray diffraction (XRD) analysis was performed to determine the mean crystallite size. The mean crystallite size was derived from Williamson Hull formula (Huang et al., 2002) that takes into account the instrumental broadening correction and the correction due to lattice strain. The magnetic properties were measured by using an Oxford Instrument Vibrating Sample Magnetometer (VSM). The electrical properties were measured by using the Magnetoresistance equipment (MR) with the method of four point probe.

3. RESULTS AND DISCUSSION

The identification results of measurements by x-ray diffraction is shown in Figure 1 in which respective profiles with milling time for 25, 50 and 75 hours are compared. In according to the Hanawalt table, samples consist of two phases, namely carbon (C) and nickel (Ni) phases. This phase result referred to the research results made by Bhattacharyya (2006) and Abrasonis (2008) for carbon and nickel phases, respectively.

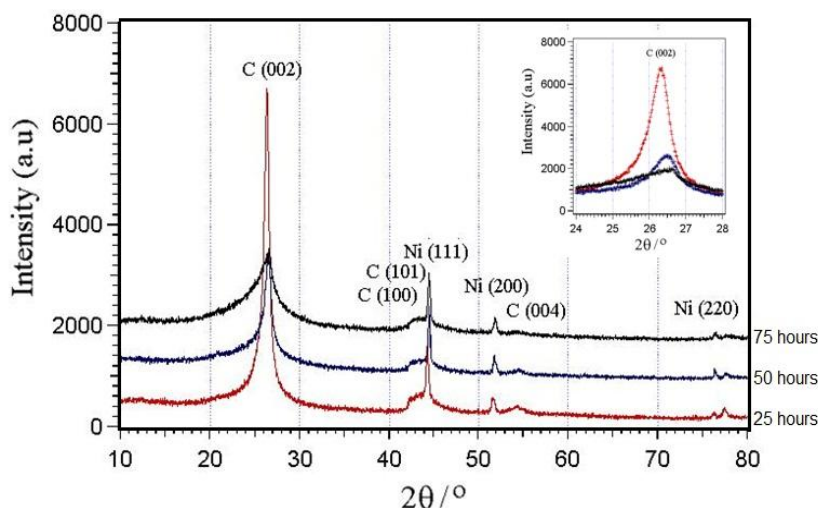


Figure 1 Phase identification of XRD on all samples

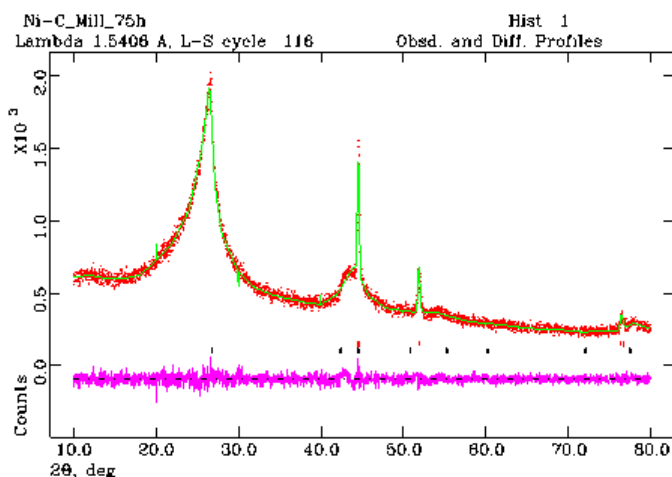


Figure 2 XRD pattern on the sample with milling time for 75 hours

Since all the samples had same composition, qualitative analysis by GSAS software is only shown on the sample with milling time for 75 hours. Figure 2 shows the refinement result of x-ray diffraction pattern on the sample with milling time for 75 hours. The quality factors of fitting on R (criteria of fit) χ^2 (goodness of fit) have been valued as the minimum, and the allowed of χ^2 is less than 1.3. There is good agreement between the observation and calculations for the profile shown in Figure 2. The refinement results of x-ray diffraction pattern show that the sample with milling time for 75 hours consist of two phases, namely carbon and nickel phases with variables, namely structure parameters, mass fraction, factor R and *goodness of fit* (χ^2) as shown in Table 1.

Table 1 Structure parameter, mass fraction, R factor and *goodness of fit* (χ^2)

Carbon (C) phase	Nickel (Ni) phase
Space group : P 63 m c (186), Hexagonal $a = b = 2.352(1) \text{ \AA}$ and $c = 6.669(7) \text{ \AA}$, $V = 31.9(7) \text{ \AA}^3$ and $\rho = 5.585 \text{ gr.cm}^{-3}$ Mass fraction = 97.33 wt%	Space group : F m -3 m (225), Cubic $a = b = c = 3.5254(7) \text{ \AA}$, $V = 43.81(2) \text{ \AA}^3$ and $\rho = 8.898 \text{ gr.cm}^{-3}$ Mass fraction = 2.67 wt%
$wRp = 4.88$ and χ^2 (chi-squared) = 1.232	

In according to the refinement result of XRD profile, it is shown that the composition of the composite samples is still suitable with preliminary composition. Figure 1 also shows that with increasing the milling time, the peak intensity of XRD profile decrease and then became broadly define. Furthermore, the crystallite size of the sample also decreased.

The crystallite size of samples could be calculated by using the Williamson Hull analysis method of X-ray diffraction. The Williamson Hull formula is defined in Equation 1 as follows:

$$FWHM(\text{rad}) \cos \theta = \frac{K\lambda}{D} + 4\varepsilon \sin \theta \tag{1}$$

which FWHM, K, λ , D, and ε are defined as full width at half maximum of the peak, Scherrer constant, X-ray wavelength, the diameter of the crystallites, and lattice strain, respectively. The calculation results of crystallite size is carried out using Williamson Hull curve as shown in Figure 3.

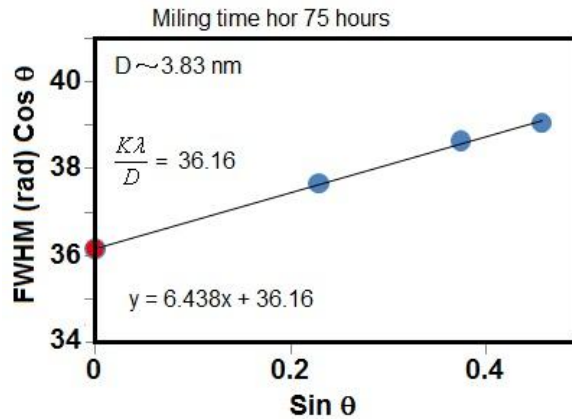


Figure 3 The crystallite size of the sample

The calculation result shows that the crystallite size of the sample (with milling time for 75 hours) was around 3.83 nm. It can be said that the milling process affects the crystallite size of the samples. In addition, the crystal size was decreased and the sample with milling time for 75 hours is also suspected to have grown embryo of carbon nanotube (CNT), due to the presence of Nickel, as shown in Figure 4. The XRD profile of the sample with milling time for 75 hours is then compared with a Multi-wall Nanotube (MWNT). Ni is the most suitable pure-metal catalyst for the growth of aligned multiwall nanotubes. This case is often found in a research about the effect of pure nickel, iron and cobalt on the growth of aligned carbon nanotubes (Huang, 2002). Carbon nanotubes grown from Ni are covered with amorphous carbon and carbon nanoparticles. The milling factor causes crystal deformation, namely crystallographic defect on the sample. The existence of crystallographic defect affect the material properties. Defects can occur in the form of atomic vacancies. A defect can cause single monoatomic vacancies that induce magnetic properties.

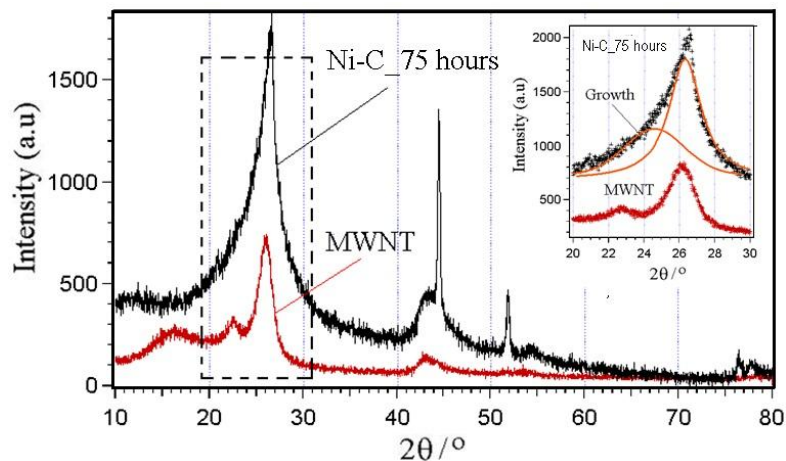


Figure 4 XRD profile of sample and MWNT

Figure 5 shows hysteresis curve of sample with milling time for 75 hours. The sample shows a ferromagnetic behavior. This is indicated by the presence of remanence and coersivity field of the magnetization curve, as a function of applied field. The hysteresis loop consists of intrinsic saturation M_s , remanence M_r , and coercivity H_c , which their values are 1.40 emu/gr, 0.28 emu/gr, and 128 Oe, respectively.

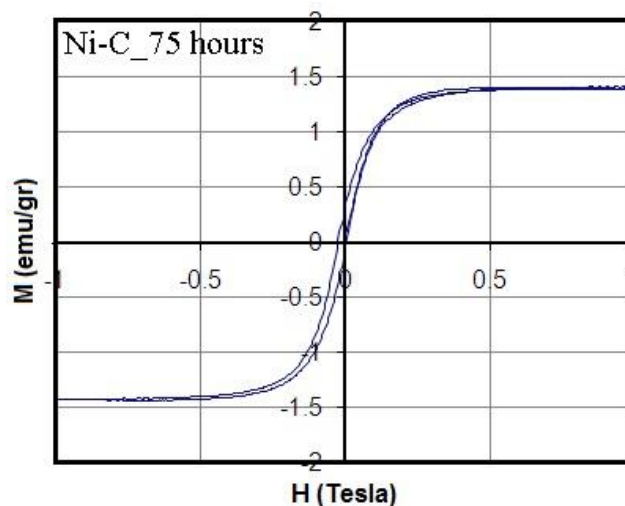


Figure 5 Hysteresis loops of the sample

Crystallographic defects also affect the electrical properties. Figure 6 show the resistivity curve as a function of the applied magnetic field on the sample with milling time for 75 hours. The phenomenon is known as magnetoresistance behavior of the sample and it define the characteristics for sensor application. Finally, an external magnetic field can be used to change the magnetic order in the sample, which can be accompanied by a drastic change in the resistance. It is clearly shown that as the external magnetic field increase, the resistivity of sample also increase. A common result is lowered conductivity through the defective region of the structure. An armchair-type defect can cause the surrounding region to become semiconducting.

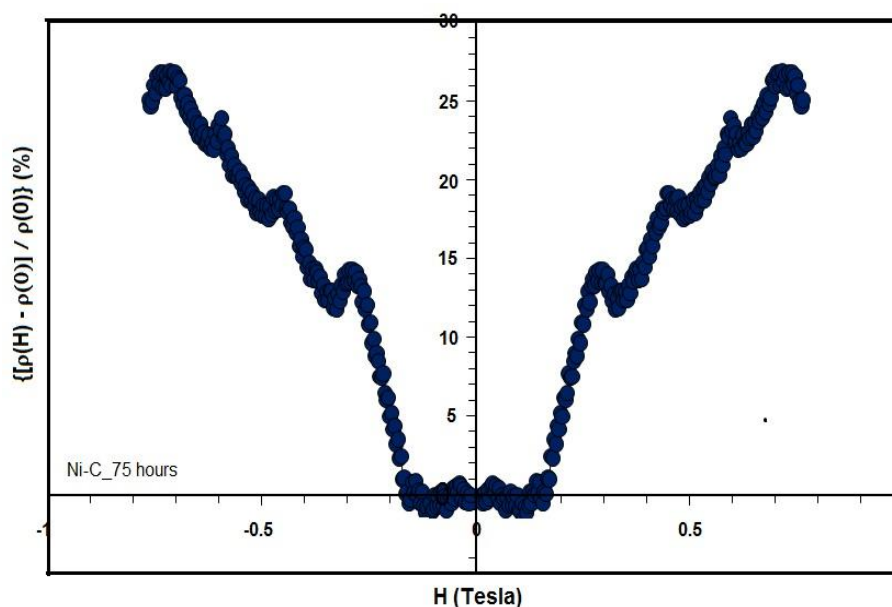


Figure 6 The resistivity curve as a function of the applied magnetic

4. CONCLUSION

The nanocomposite Ni-C has been successfully made by mechanical milling method. The sample consist of two phases, namely carbon and nickel phases. Carbon phase has hexagonal structure, space group: P 63 m c (186), lattice parameters of $a = b = 2.352(1) \text{ \AA}$ and $c =$

6.669(7) Å, Å, $\alpha = \beta = 90^\circ$ and $\gamma = 120^\circ$, $V = 31.9(7) \text{ \AA}^3$ and $\rho = 5.585 \text{ gr.cm}^{-3}$. Nickel phase has cubic structure, Space group: $Fm\bar{3}m$ (225), lattice parameters of $a = b = c = 3.5254(7) \text{ \AA}$, $\alpha = \beta = \gamma = 90^\circ$, $V = 43.81(2) \text{ \AA}^3$ and $\rho = 8.898 \text{ gr.cm}^{-3}$. The calculation result shows that the crystallite size of the sample with milling time for 75 hours was around 3.83 nm. The sample with milling time for 75 hours is also suspected to have grown embryo of carbon nanotube (CNT), due to the presence of nickel. The hysteresis loop of the sample consists of intrinsic saturation M_s , remanence M_r , and coercivity H_c are 1.40 emu/gr, 0.28 emu/gr, and 128 Oe, respectively. The value of magnetoresistance is about 28% at 7.5 kOe magnetic field. The sample shows the magnetoresistance behavior and the phenomenon of sensor characteristic.

5. ACKNOWLEDGMENT

This work was supported by the program for research and development of giant magnetoresistance (GMR) materials for biosensors (DIPA 2014), Center for Science and Technology of Advanced Materials, National Nuclear Energy Agency, Indonesia.

6. REFERENCES

- Abrasonis, G., Scheinost, A.C., Zhou, S., Torres, R., Gago, R., Jiménez, I., Kuepper, K., Potzger, K., Krause, M., Kolitsch, A., Möller, W., Bartkowski, S., Neumann, M., Gareev R.R., 2008. X-ray Spectroscopic and Magnetic Investigation of C:Ni Nanocomposite Films Grown by Ion Beam Cosputtering. *J. Phys. Chem. C*, Volume 112, pp. 12628–12637
- Bhattacharyya, S., Henley, S.J., Lock, D., Blanchard, N.P., Silva, S.R.P., 2006. Semiconducting Phase of Amorphous Carbon-nickel Composite Films. *Appl. Phys.*, Volume 89, pp. 1–3
- Cernak, J., Helgesen, G., Hage, F.S., Kovac, J., 2014. Magnetoresistance of Composites based on Graphitic Discs and Cones. *J. Phys. D: Appl. Phys.*, Volume 47, pp. 2–17
- Dillon, F.C., Bajpai, A., Koo's, A., Downes, S., Aslam, Z., Grobert, N., 2012. Tuning the Magnetic Properties of Iron-filled Carbon Nanotubes. *Carbon*, Volume 50, pp. 3674–3681
- Guler, O., Evin, E., 2012. Carbon Nanotube Formation by Short Time Ball Milling and Annealing of Graphite. *J. Optoelectron. Adv. Mater., Rapid Commun.*, Volume 6, pp. 183–187
- Huang, Z.P., Wang, D.Z., Wen, J.G., Sennett, M., Gibson, H., Ren, Z.F., 2002. Effect of Nickel, Iron and Cobalt on Growth of Aligned Carbon Nanotubes. *Appl. Phys. A*, Volume 74, pp. 387–391
- Jia, B., Su, L., Han, G., Wang, G., Zhang, J., Wang, L., 2011. Adsorption Properties of Nickel-based Magnetic Activated Carbon Prepared by Pd-free Electroless Plating. *BioResources*, Volume 6, pp. 70–80
- Mandal, G., Srinivas, V., Rao, V.V., 2013. Role of Particle Size on the Magnetoresistance of Nano-crystalline Graphite. *Carbon*, Volume 57, pp. 139–145
- Sagar, R.U., Zhang, X., Xiong, C., Yu, Y., 2014. Semiconducting Amorphous Carbon Thin Films for Transparent Conducting Electrodes. *Carbon*, Volume 76, pp. 64–70
- Schinteie, G., Kuncser, V., Palade, P., Dumitrache, F., Alexandrescu, R., Morjan, I., Filoti, G., 2013. Magnetic Properties of Iron-carbon Nanocomposites Obtained by Laser Pyrolysis in Specific Configurations. *Journal of Alloys and Compounds*, Volume 564, pp. 27–34
- Toby, B.H., 2000. EXPGUI, a Graphical User Interface for GSAS. *J. Applied Crystallography*, Volume 34, pp. 210–213
- Venkatesan, M., Dunne, P., Chen, Y.H., Zhang, H.Z., Coey, J.M.D., 2013. Structural and Magnetic Properties of Iron in Graphite. *Carbon*, Volume 56, pp. 279–287
- Xu, Y., Zhang, D., Cai, J., Yuan, L., Zhang, W., 2012. Effects of Multi-walled Carbon Nanotubes on the Electromagnetic Absorbing Characteristics of Composites Filled with Carbonyl Iron Particles. *J. Mater. Sci. Technol.*, Volume 28, pp. 34–40

- Yunasfi, 2013. Effects of Milling Time on Magnetic Properties of Ni-C Composites. *Scientific Publication Journal of Instrumentasi*, Volume 37, pp. 19–24
- Zou, T., Li, H., Zhao, N., Shi, C., 2010. Electromagnetic and Microwave Absorbing Properties of Multi-walled Carbon Nanotubes Filled with Ni Nanowire. *Journal of Alloys and Compounds*, Volume 496, pp. 22–24